

Article

Patchouli Alcohol: A Potent Tyrosinase Inhibitor Derived from Patchouli Essential Oil with Potential in the Development of a Skin-Lightening Agent

K. J. Senthil Kumar ^{1,2,*}, M. Gokila Vani ³, Muthusamy Chinnasamy ⁴, Wan-Teng Lin ⁵ and Sheng-Yang Wang ^{3,6}

¹ Bachelor Program of Biotechnology, National Chung Hsing University, Taichung 402, Taiwan

² Center for General Education, National Chung Hsing University, Taichung 402, Taiwan

³ Department of Forestry, National Chung Hsing University, Taichung 402, Taiwan; mgvani2009@gmail.com (M.G.V.); taiwanfir@dragon.nchu.edu.tw (S.-Y.W.)

⁴ Department of Biotechnology, Srinivasan College of Arts and Science, Perambalur 621212, Tamil Nadu, India; biotech@scas.ac.in

⁵ Department of Hospitality Management, College of Agriculture and Health, Tunghai University, Taichung 40704, Taiwan; 040770@thu.edu.tw

⁶ Agricultural Biotechnology Research Center, Academia Sinica, Taipei 11529, Taiwan

* Correspondence: zenkumar@dragon.nchu.edu.tw; Tel.: +886-4-22840811 (ext. 537)

Abstract: The inhibitory effects of *Pogostemon cablin* essential oil (patchouli essential oil, PEO) and its primary bioactive compound, patchouli alcohol (PA), on tyrosinase and melanin were investigated in vitro and ex vivo. Treatment with PEO and PA significantly, as well as dose-dependently, reduced forskolin (FRK)-induced melanin biosynthesis, cellular tyrosinase activity, and tyrosinase (TYR) protein expression. However, the transcriptional levels of TYR and tyrosinase-related proteins (TRP-1 and TRP-2) remained unaffected. These results suggest that PEO and PA may directly interrupt tyrosinase enzyme activity, leading to a reduction in melanin biosynthesis. Further experiments supported this notion, revealing that both PEO and PA significantly and dose-dependently inhibited mushroom tyrosinase activity in both the monophenolase and diphenolase phases. Additionally, an in silico molecular docking analysis was performed, utilizing a homology model of human tyrosinase. In conclusion, these findings strongly suggest that patchouli essential oil and its primary bioactive component, patchouli alcohol, hold promise as potential treatments for hyperpigmentary skin conditions and in the development of cosmetic products designed to lighten the skin.

Keywords: *Pogostemon cablin*; patchouli oil; patchouli alcohol; tyrosinase; melanin; skin whitening



Citation: Kumar, K.J.S.; Vani, M.G.; Chinnasamy, M.; Lin, W.-T.; Wang, S.-Y. Patchouli Alcohol: A Potent Tyrosinase Inhibitor Derived from Patchouli Essential Oil with Potential in the Development of a Skin-Lightening Agent. *Cosmetics* **2024**, *11*, 38. <https://doi.org/10.3390/cosmetics11020038>

Academic Editors: João Miguel F. Rocha, Nouredine El Aouad and Jackson Roberto Guedes da Silva Almeida

Received: 4 January 2024

Revised: 18 February 2024

Accepted: 23 February 2024

Published: 5 March 2024



Copyright: © 2024 by the authors. Licensee MDPI, Basel, Switzerland. This article is an open access article distributed under the terms and conditions of the Creative Commons Attribution (CC BY) license (<https://creativecommons.org/licenses/by/4.0/>).

1. Introduction

Skin whitening and depigmentation practices are prevalent in specific ethnic groups, notably in Asia, Africa, and the Middle East. This widespread phenomenon can be attributed to the intricate interplay of cultural, social, political, and psychological factors [1]. Among Asian women, the popularity of skin-lightening products has significantly increased, driven largely by their desire to counter color-based discrimination [2]. Globally, there is a rapid demand for combination skin-lightening products. It has been estimated that their market value will reach USD 7.68 billion by 2028, with a projected growth rate of 6.23% from 2021 to 2028 [3].

Whitening is the process of reducing the amount of melanin, or pigment, in the skin to make it appear lighter. Melanin is part of a group of natural pigments that is ubiquitous in nearly all living organisms, playing an essential role in epidermal homeostasis and serving as a defense against environmental stressors, such as ultraviolet radiation from the sun [4]. In contrast, abnormal melanin synthesis can be associated with various dermatological conditions, including the formation of freckles, solar lentigo, melasma, vitiligo, melanoma,

and other hyperpigmented skin disorders [5]. Hyperpigmentation-related skin disorders can be treated with depigmentation agents, including conditions such as melasma, post-inflammatory hyperpigmentation, congenital melanocytic naevi, lentigo, erythromelanosis follicularis faciei et colli, and erythema dyschromicum perstans [6].

The overproduction of melanin by the melanosomes leads to hyperpigmentation, a result of melanogenesis. These processes begin when L-tyrosine is converted into three major types of pigments, including eumelanin, pheomelanin, and mixed melanin [7]. Tyrosinase (TYR) plays a crucial role in melanogenesis, catalyzing the initial two stages involved in the conversion of L-tyrosine into L-DOPA and the subsequent conversion of L-DOPA into dopaquinone. Additionally, tyrosinase-related protein-1 (TYRP-1) and tyrosinase-related protein-2 (TRP-2), also known as dopachrome tautomerase (DCT), are the enzymes specifically involved in eumelanin biosynthesis. TYRP-2 catalyzes the tautomerization of dopachrome to 5,6-dihydroxyindole-2-carboxylic acid (DHICA). This compound is subsequently converted into eumelanin by TYRP-1 [8]. Therefore, the identification of tyrosinase inhibitors has been the most frequently used approach for suppressing or reducing melanogenesis, or for skin whitening [7].

Numerous studies have documented the presence of TYR inhibitors in natural sources, with the majority being identified in plants. Skin-whitening agents sourced from nature hamper melanin biosynthesis by directly suppressing TYR activity. They also disturb the melanin synthesis cascade, affecting pathways such as the microphthalmia-associated transcription factor (MITF) pathway [9]. MITF, a pivotal basic helix-loop-helix leucine zipper transcription factor, plays a crucial role in the regulation of genes within the tyrosinase and tyrosinase-related proteins family in melanocytes. Various reports indicate that natural products deregulate the MITF pathway during stimulated melanin synthesis in melanocytes. They also suppress melanosome's uptake and distribution in keratinocytes [9]. Commonly utilized in cosmetics and dermatology, whitening agents include arbutin, azelaic acid, hydroquinone, kojic acid, and resveratrol. Despite their efficacy, each of these agents raises safety concerns [10]. Many skin-whitening products contain ingredients that are toxic when used cosmetically for extended periods without medical guidance. These ingredients not only have the potential to harm the skin but also to cause life-threatening illnesses [10]. For instance, hydroquinone, a natural phenolic compound considered the gold standard for skin whitening, has been used for decades. However, its long-term use has been associated with various adverse effects, including contact dermatitis, conjunctival melanosis, corneal degeneration, exogenous ochronosis, nail discoloration, and skin irritation. Moreover, it has been shown to be toxic to the kidneys, bone marrow, and the immune system [1]. Furthermore, in the European Union (EU), hydroquinone has been regulated, with restrictions imposed on its use in cosmetic products due to concerns about the carcinogenicity of its metabolite. Another natural whitening agent, kojic acid, is known for its storage stability issues and carcinogenic activity [1]. Several natural tyrosinase activity inhibitors have proven ineffective in human applications due to their low bioavailability. Consequently, researchers in academia and in industry are actively exploring novel potent and safe tyrosinase inhibitors from both natural and synthetic sources.

Patchouli essential oil (PEO) is a volatile extract obtained from the dried leaves of *Pogostemon cablin* (Blanco) Benth. (Lamiaceae) through steam distillation or hydrodistillation methods. Renowned for its distinctive woody aroma, it stands as a key ingredient in perfumery, cosmetics, toiletries, detergents, and the pharmaceutical industry [11]. Indeed, it has been emphasized that "patchouli oil is one of the most crucial materials available to the perfumer". Significant research has been conducted on the chemical constituents and bioactivities of patchouli oil [11]. Patchouli alcohol (syn. patchoulol), a tricyclic sesquiterpene, has emerged as a significant bioactive component in the oil extracted from the aerial parts of *P. cablin*. Prior investigations have documented the broad spectrum of bioactivities associated with patchouli alcohol, including anti-influenza virus, anti-depressive, anti-nociceptive, vasorelaxation, lung protection, brain protection, anti-ulcerogenic, anti-colitis, prebiotic-like, anti-inflammatory, anti-cancer, and protective activities against metabolic

diseases [12]. Up to this point, there have been no reported findings concerning the potential skin-whitening effects of either patchouli oil or its primary bioactive compound, patchouli alcohol. The present study aims to investigate the anti-melanogenic properties of patchouli essential oil and patchouli alcohol utilizing a murine melanoma cell model.

2. Materials and Methods

2.1. Chemicals and Reagents

Patchouli essential oil (PEO) was provided by Bio-Jourdeness International Groups Co., Ltd. (Taichung, Taiwan). Patchouli alcohol was obtained from Biosynth International, Inc. (San Diego, CA, USA). The compound's purity was determined to be above 99%, as confirmed by both gas chromatography (GC) and proton nuclear magnetic resonance ($^1\text{H-NMR}$) analyses. Fetal bovine serum (FBS), Roswell park memorial institute (RPMI) 1640 medium, penicillin, and streptomycin were procured from Life Technologies (Grand Island, NY, USA). 3-(4,5-dimethyl-thiazol-2-yl)-2,5-diphenyl tetrazolium bromide (MTT), tyrosinase (EC 1.14.18.1, activity of 6680 units/mg), melanin, and kojic acid (KA) were purchased from Sigma-Aldrich (St. Louis, CA, USA). Forskolin (FRK) was acquired from Selleckchem (Houston, TX, USA). An antibody against tyrosinase was obtained from Genetex, Irvin, CA, USA. Antibodies against GAPDH, tyrosinase-related protein-1, and tyrosinase-related protein-2 were obtained from Santa-Cruz Biotechnology (Dallas, TX, USA). Horseradish peroxidase (HRP)-linked anti-mouse IgG and anti-rabbit IgG antibodies were sourced from Cell Signaling Technology (Danvers, MA, USA). All other chemicals used were of reagent grade or HPLC grade and were provided by either Merck (Darmstadt, Germany) or Sigma-Aldrich.

2.2. Cell Culture and Cell Viability Assay

The murine melanoma (B16-F10) cell line was procured from the American Type Culture Collection (ATCC, Manassas, VA, USA). Cells were cultured in RPMI-1640 medium supplemented with glucose, penicillin, and streptomycin, and 10% FBS. They were grown in 10 cm culture dishes and incubated in a humidified atmosphere containing 5% CO_2 at 37 °C. The sub-culturing of cells was performed at three-day intervals. Cell viability was assessed using the MTT colorimetric assay. B16-F10 cells were seeded in a 96-well plate at a density of 1×10^4 cells/well. After 24 h of incubation, cells were treated with various concentrations (25, 50, 100, 150, and 200 $\mu\text{g}/\text{mL}$) of PEO or 25–100 μM PA or 20 μM FRK for an additional 48 h. Control cells were treated with 0.1% DMSO/RPMI for 48 h. After removing the cell culture supernatant, 1 mg/mL of MTT in 200 μL of fresh culture medium was added. The resulting MTT formazan crystals were dissolved in 200 μL of DMSO. Subsequently, the samples were measured at 570 nm (A_{570}) using an ELISA microplate reader (Bio-Tek Instruments, Winooski, VT, USA). The percentage of cell viability was determined using the following formula: (A_{570} of treated cells/ A_{570} of untreated cells) \times 100.

2.3. Determination of Melanin Content and Cellular Tyrosinase Activity

Melanin content and cellular tyrosinase activity were assessed following previously established procedures [13]. In brief, B16-F10 cells were seeded in 6 cm cell culture dishes at a density of 1×10^5 cells/dish. When the cell confluence reached 50%, cells were treated with FRK at a concentration of 20 μM , either in the presence or absence of PEO at concentrations ranging from 25 to 100 $\mu\text{g}/\text{mL}$, or PA (25–100 μM), or KA (20 μM), for a duration of 48 h. Subsequently, the cells were harvested, washed twice with PBS, and the intracellular melanin was solubilized in 1N NaOH, and then incubated at 68 °C for 20 min. The melanin content was quantified by measuring the absorbance at 475 nm using an ELISA microplate reader. In another set of experiments, cells were subjected to similar conditions for 48 h. Cultured cells were lysed with a lysis buffer and subsequently clarified by centrifugation at $16,000 \times g$ for 10 min. A total of 90 μL from each lysate, containing an equal amount of protein (100 μg), was dispensed into a 96-well plate. Subsequently,

10 μ L of 15 mM L-DOPA was introduced to each well. Following an incubation period, at 37 °C, of 20 min, the formation of dopachrome was quantified at 475 nm using an ELISA microplate reader.

2.4. Protein Extraction and Western Blot Analysis

Cell lysis was performed using radioimmunoprecipitation assay buffer (RIPA buffer, Pierce Biotechnology, Rockford, IL, USA). Protein concentrations were determined using the Bio-Rad protein assay reagent (Bio-Rad Laboratories, Hercules, CA, USA), which is based on the Bradford dye-binding method. Subsequently, equal amounts of the protein samples (100 μ g) were subjected to separation by 8–12% SDS-PAGE, and the separated proteins were transferred onto a polyvinylidene fluoride (PVDF) membrane. After transfer, the protein membranes were blocked with 5% non-fat skim milk for 30 min, followed by an overnight incubation with specific primary antibodies. Subsequently, the membranes were probed with HRP-conjugated anti-rabbit or anti-mouse antibodies for 2 h. Immunoblots were visualized using enhanced chemiluminescence (ECL) reagents (Advansta Inc., San Jose, CA, USA), and the ChemiDoc XRS⁺ docking system was employed to capture images. Quantitative analysis of the protein bands was conducted using Imagelab software version 6.0.1 from Bio-Rad Laboratories.

2.5. Immunofluorescence and Fluorescence Microscopy

B16–F10 cells (2×10^4 cells/well) were cultured on Nunc Lab-Tek[®] cell culture slides (ThermoFisher Scientific, Waltham, MA, USA) and subjected to treatment with FRK, with or without PA (100 μ M) or KA (50 μ M), for 24 h. Following treatment, the culture media were aspirated, and the cells were fixed in 2% paraformaldehyde for 15 min. Following fixation, the cells were permeabilized with 0.1% Triton X-100 for 10 min, washed, and then blocked with 10% FBS in PBS. Following this, the cells were incubated for 2 h with anti-tyrosinase antibody in 1.5% FBS. The cells were subsequently incubated with the fluorescein isothiocyanate (FITC)-conjugated secondary antibody for an additional 1 h in 6% bovine serum albumin (BSA). Following that, the cells were stained with 1 μ g/mL of DAPI for 5 min, washed with PBS, and visualized using a fluorescence microscope (Olympus Corp., Tokyo, Japan) at 20 \times magnification.

2.6. RNA Extraction and q-PCR Analyses

Total RNA extraction was performed using the GeneMark Total RNA Purification Kit (GeneMark, New Taipei City, Taiwan), following two washes of the B16–F10 cells with cold PBS. The SuperScript[™] IV First-Strand Synthesis Kit (Invitrogen, Waltham, MA, USA) was utilized to convert 2 μ g of extracted RNA into cDNA. Subsequently, mRNA expression levels were quantified using the Applied Biosystems Real-Time PCR System (Applied Biosystems, Waltham, MA, USA) and Power SYBR Green Master Mix (Applied Biosystems). The amplification process was conducted under the following conditions: the qPCR reaction involved an initial denaturation step at 96 °C for 3 min, followed by 40 cycles of denaturation at 96 °C for 1 min, annealing at 50 °C for 30 s, and extension at 72 °C for 90 s. The primer sequences for each gene in the qPCR were as follows: *TYR*—forward primer (F), 5'-TATTGAGCCTTACTTGGAAC-3'; reverse primer (R), 5'-AAATAGGTCGAGTGAGGTAA-3', *TRP-1*—forward primer (F), 5'-TGCAGGAGCCTTCTTTCTC-3'; reverse primer (R), 5'-AAGACGCTGCACTGCTGGTCT-3', *TRP-2*—forward primer (F), 5'-GGATGACCGTGAGC AATGGCC-3'; reverse primer (R), 5'-CGGTTGTGACCAATGGGTGCC-3', and *GAPDH*—forward primer (F), 5'-TCAACGGCACAGTCAAGG-3'; reverse primer (R), 5'-ACTCCACG ACATACTCAGC-3'. The copy number for each transcript was determined by calculating the relative copy number, which was normalized to the GAPDH copy number. The relative abundance of the target mRNA in each sample was calculated based on the Δ Ct values of the target and the endogenous reference gene GAPDH, employing the $2^{\Delta\Delta}$ Ct cycle threshold method.

2.7. Mushroom Tyrosinase Activity Inhibition Assay

The *ex vivo* mushroom tyrosinase assay utilized L-tyrosine and L-DOPA as substrates for tyrosinase activity. The inhibitory activity of PEO and PA against the tyrosinase-catalyzed oxidation of L-tyrosine was determined following the method outlined by Chang [14]. In brief, a 40 μL volume of 1.5 mM substrate (L-tyrosine) dissolved in 0.1 M phosphate buffer (pH 6.8) was combined with 120 μL of 0.1 M phosphate buffer. To this mixture, 20 μL of different concentrations of PEO (12.5–100 $\mu\text{g}/\text{mL}$) or PA (12.5–100 μM) were added. Following this, 20 μL of mushroom tyrosinase (2000 U/mL in phosphate buffer) was introduced to initiate the reaction. The assay mixture was then incubated at 37 $^{\circ}\text{C}$ for 15 min. A microplate reader (μQuant , BioTek Instruments, Winooski, VA, USA) was employed to monitor the increase in absorbance at 475 nm, indicative of dopachrome formation. The inhibitory effect of PEO and PA on mushroom tyrosinase in L-DOPA oxidation was assessed. A mixture of 100 μL of 0.1 M phosphate buffer and 20 μL of different concentrations of POE (5–100 $\mu\text{g}/\text{mL}$) or PA (12.5–100 μM) was prepared. Following that, 20 μL of mushroom tyrosinase (2000 U/mL in phosphate buffer) was added to initiate the reaction. The mixture was then incubated at 37 $^{\circ}\text{C}$ for 5 min before introducing 40 μL of L-DOPA (4 mM in 0.1 M of phosphate buffer). Subsequently, the mixture underwent incubation for an additional 10 min at 37 $^{\circ}\text{C}$, and the absorbance, at 475 nm, of the reaction mixture was recorded. As a positive control, kojic acid (40 μM) was employed for the assay. The percentage inhibition of L-tyrosine or L-DOPA oxidation was calculated using the following formula: % inhibition = $100 - (B/A \times 100)$, where $A = \Delta\text{OD}_{475}$ over 10 min without the sample, and $B = \Delta\text{OD}_{475}$ over 10 min with the tested sample.

2.8. In Silico Molecular Docking Study

2.8.1. Ligand and Receptor Selection

In this study, a total of 9 aromatic organic compounds were selected as ligands for *in silico* molecular docking study. Three-dimensional structures of all the selected ligands were downloaded from <https://pubchem.ncbi.nlm.nih.gov> accessed on 19 October 2023. The list of ligands is α -bulnesene, α -guaiene, azulene, β -patchoulene, δ -guaiene, δ -patchoulene, patchouli alcohol, and seychellene. The predicted 3D structure of the human tyrosinase receptor, generated by alpha-Fold, was obtained from <https://www.uniprot.org> with the molecular ID AF-L8B082-F1 was accessed on 2 September 2023. During processing, residues with a confidence score below 70 were excluded, and the core structure was utilized for the docking study.

2.8.2. Prediction of Ligand and Protein Interaction

We used Schrodinger 2023-3 software to prepare and optimize the structure of the protein, using the OPLS_2005 force field to remove heteroatoms (Schrodinger, LLC, New York, NY, USA). The binding site of the protein structure was identified using SitMap (Sitemap, Version 4.3), available in Maestro, and some other physical characteristics such as hydrogen bonding, hydrophobicity, size, and linking point [15]. A grid created at 12 $\text{\AA} \times 12 \text{\AA} \times 12 \text{\AA}$ was virtually screened and run in VSW (virtual screening workflow module). Then, the virtual screening workflow was performed in QikProp (ligand filter), LigPrep, and glide docking (HTVS, SP, and XP).

2.9. Statistical Analysis

The data are presented as mean \pm SD. Statistical analysis was conducted using GraphPad Prism version 6.0 for Windows (GraphPad Software, La Jolla, CA, USA). A one-way ANOVA followed by Dunnett's test for multiple comparisons was employed for statistical evaluation. p values of less than 0.05 *, 0.01 **, and 0.001 *** were considered statistically significant for the FRK treatment vs. the PEO or PA or KA treatment groups. Additionally, p values of less than 0.01 $^{\Delta}$ were considered statistically significant for the FRK treatment vs. the control group.

3. Results

3.1. PEO Inhibits Melanin Biosynthesis in FRK-Induced B16-F10 Cells

Before exploring the anti-melanogenic properties of PEO, we assessed its cytotoxic effects on B16-F10 murine melanoma cells. As shown in Figure 1A, the 48 h treatment with PEO does not exhibit cytotoxicity against B16-F10 cells, even at the highest treatment dose of 100 $\mu\text{g}/\text{mL}$. However, concentrations exceeding 100 $\mu\text{g}/\text{mL}$ induced cytotoxicity in melanoma cells. Given that the murine melanoma cells showed no cytotoxicity when treated with PEO up to a dosage of 100 $\mu\text{g}/\text{mL}$, we have refrained from verifying its cytotoxic effects in other dermal cell lines. Hence, in subsequent experiments, we employed non-cytotoxic concentrations within the range of 25 to 100 $\mu\text{g}/\text{mL}$. Following that, we assessed the inhibitory effect of PEO on FRK-induced melanin synthesis in melanoma cells. The result of the melanin content assay is shown in Figure 1B. The cellular melanin content in FRK-stimulated cells exhibited a significant increase from 2.5 $\mu\text{g}/\text{mL}$ to 7.44 $\mu\text{g}/\text{mL}$, whereas co-treatment with PEO reduced melanin synthesis compared to only FRK-stimulated cells in a significant and dose-dependent manner. The reduction was observed at concentrations of 5.14 $\mu\text{g}/\text{mL}$, 3.60 $\mu\text{g}/\text{mL}$, and 2.14 $\mu\text{g}/\text{mL}$ with PEO doses of 25 $\mu\text{g}/\text{mL}$, 50 $\mu\text{g}/\text{mL}$, and 100 $\mu\text{g}/\text{mL}$, respectively. Indeed, the 100 $\mu\text{g}/\text{mL}$ PEO treatment remarkably reduced the content of cellular melanin, which was comparatively lower than that of the basal level. Moreover, the melanin synthesis inhibitory effect of PEO is remarkably comparable to the well-known melanin synthesis inhibitor kojic acid (KA, 40 μM), which demonstrated a reduction at 5.26 $\mu\text{g}/\text{mL}$. This is 3-fold higher than the melanin synthesis inhibition observed with 100 $\mu\text{g}/\text{mL}$ of PEO (2.14 $\mu\text{g}/\text{mL}$). The aforementioned effect was additionally validated through FM staining. As demonstrated in Figure 1C, in comparison to the control cells, cells treated with FRK exhibited a substantial increase in Fontana–Masson staining, which serves as an indicator of the melanin content. Cells treated with either PEO or KA exhibited reduced FM staining, which can be attributed to their low levels of intracellular melanin.

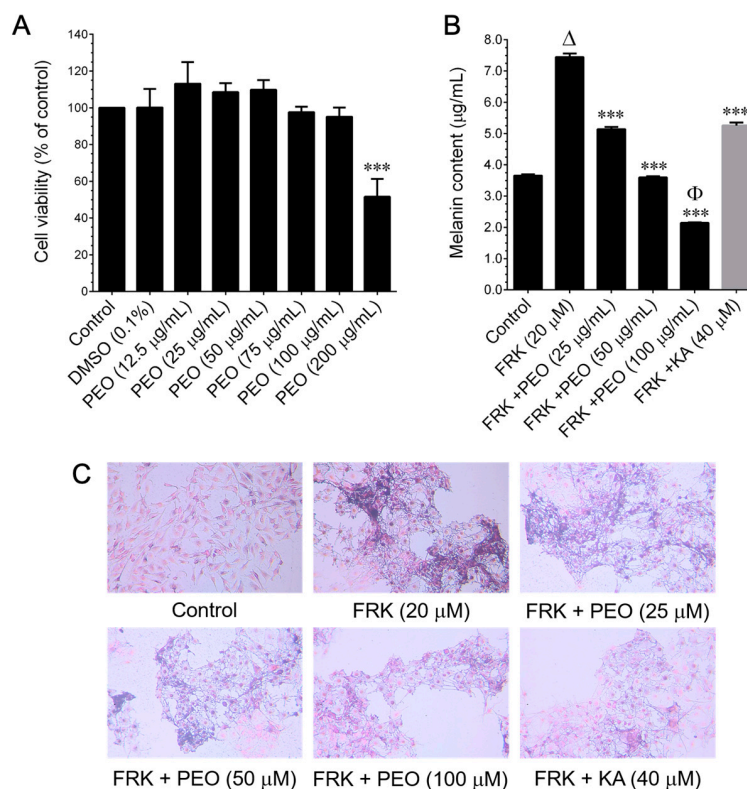


Figure 1. The effects of PEO on melanin synthesis in melanoma cells. (A) Cells were incubated with increasing doses of PEO (12.5–200 $\mu\text{g}/\text{mL}$) for 48 h, and cell viability was assessed using the MTT

colorimetric assay. The results, presented as the mean \pm SD of three independent experiments, indicate statistical significance (** $p < 0.001$) when comparing the control to the PEO treatment groups. (B) Cells were treated with escalating doses of PEO (25–100 $\mu\text{g}/\text{mL}$) or KA (40 μM) in the presence of 20 μM FRK for 48 h, and their melanin content was quantified from their total cell lysates. (C) Following a 48 h treatment with PEO and FRK, cells were stained using Fontana–Masson staining to visualize their subcellular melanin content. The data, representing the mean \pm SD of three independent experiments, indicate statistical significances: $\Delta p < 0.01$ of the control vs. FRK; $\Phi p < 0.01$ between the PEO and FRK control groups; and ** $p < 0.001$ between the PEO/KA and FRK treatment groups. Dimethyl sulfoxide (DMSO), patchouli essential oil (PEO), forskolin (FRK), and kojic acid (KA).

3.2. PEO Inhibits FRK-Induced Cellular Tyrosinase Activity and Expression

In order to examine the mechanism by which PEO reduces the melanin biosynthesis in B16–F10 cells, we assessed cellular tyrosinase activity, a pivotal factor in melanin biosynthesis. As shown in Figure 2A, there was a significant increase in cellular tyrosinase activity to 223.5% upon FRK stimulation. However, co-treatment with PEO resulted in a reduction in cellular tyrosinase activity to 209.4%, 186.3%, and 146.6% at concentrations of 25, 50, and 100 $\mu\text{g}/\text{mL}$, respectively. Furthermore, PEO demonstrated an equivalent inhibitory potency to kojic acid (KA). The results indicate that PEO exerts a potent inhibitory effect on intracellular tyrosinase activity. To gain a deeper understanding of PEO's inhibitory effect on melanin biosynthesis and tyrosinase activity, we aimed to assess the effect of PEO on the regulatory proteins of melanogenesis. This included examining the levels of tyrosinase (TYR), TRP-1, and TRP-2 present through immunoblotting. As shown in Figure 2B–E, upon FRK stimulation, the expression of tyrosinase significantly increased by 6.1-fold compared to control cells. However, co-treatment with PEO markedly reduced tyrosinase expression, almost reaching basal levels (1.37-fold) at a dose of 100 $\mu\text{g}/\text{mL}$. In contrast, FRK-treated cells exhibited a significant increase in TRP-1, while co-treatment with PEO failed to modulate TRP-1 expression at lower concentrations. However, a significant increase was observed at the higher concentration of 100 mg/mL . Additionally, neither FRK nor PEO altered the protein expression levels of TRP-2 in B16–F10 cells. To further elucidate the mechanism behind the down-regulation of tyrosinase protein expression by PEO, we proceeded to assess the level of tyrosinase, TRP-1, and TRP-2 mRNA expression in B16–F10 cells through q-PCR analysis. As shown in Figure 2F–H, in FRK-stimulated cells, the mRNA expression levels of tyrosinase, TRP-1, and TRP-2 were significantly elevated to 5.20-fold, 3.66-fold, and 2.05-fold, respectively. Surprisingly, co-treatment with PEO did not alter their mRNA expression levels at any of the tested doses. These results suggest that the reduction in cellular tyrosinase activity by PEO may directly interrupt tyrosinase activity rather than modulating its signaling pathway.

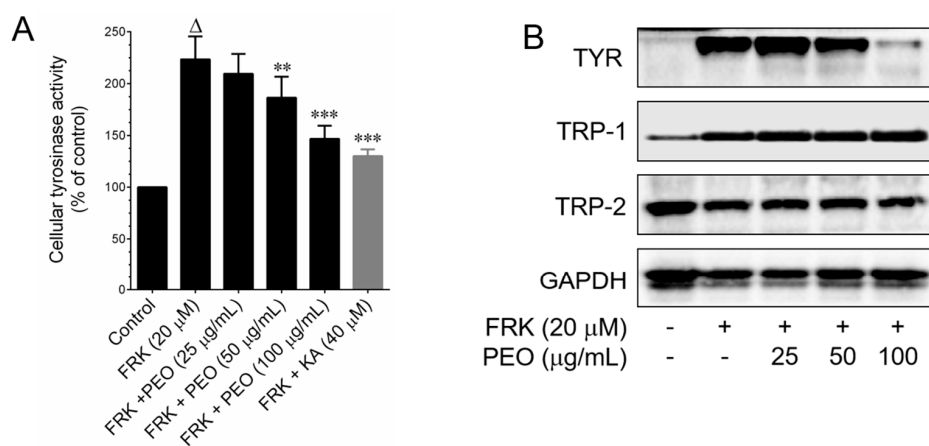


Figure 2. Cont.

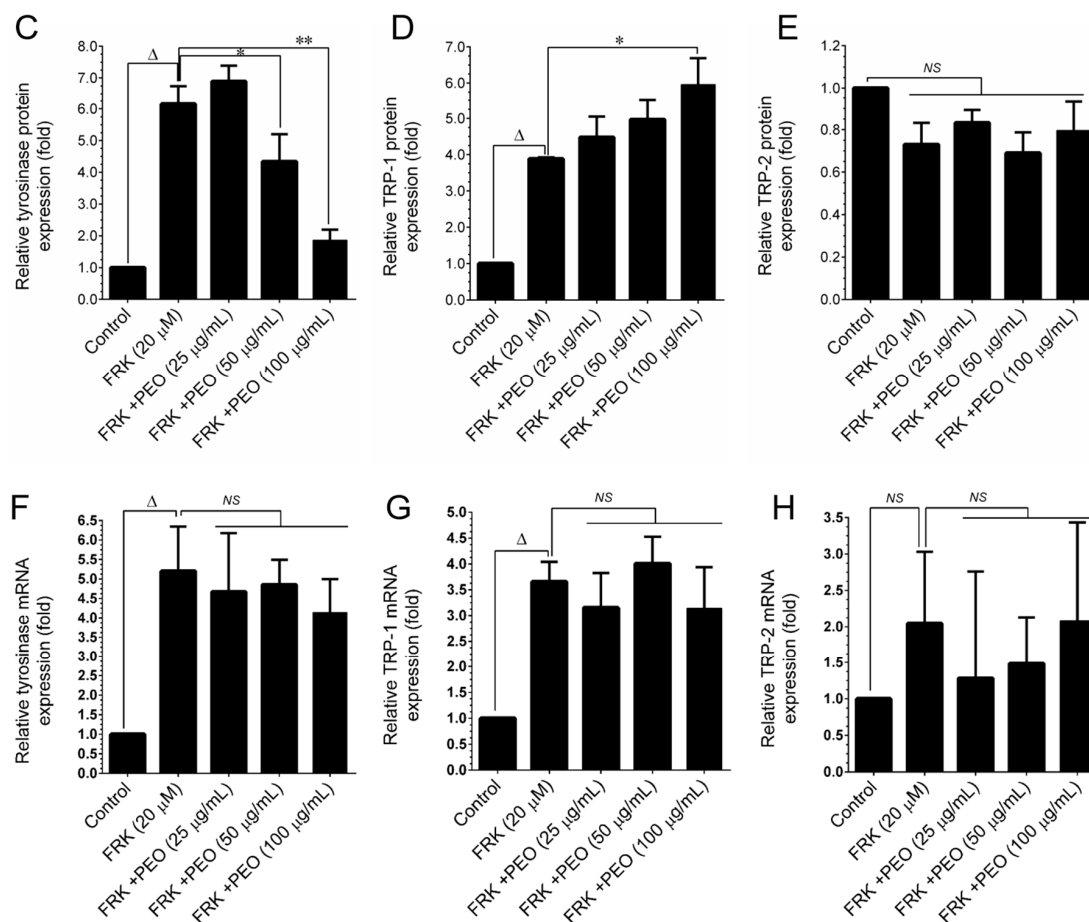


Figure 2. The effect of PEO on FRK-induced cellular tyrosinase and melanogenesis regulatory proteins in B16-F10 cells. Cells were treated with increasing concentrations of PEO or KA and stimulated with FRK for 48 h. (A) Enzymatic measurement of cellular tyrosinase activity was performed using L-DOPA as a substrate, and the effects on L-DOPA oxidation velocity were measured at 492 nm. (B–E) Western blot analysis determined the protein expression levels of tyrosinase (TYR), TRP-1, and TRP-2. The histogram illustrates the relative protein expression, normalized with the loading control GAPDH. (F–H) q-PCR analysis assessed the relative mRNA expression levels of tyrosinase, TRP-1, and TRP-2. The data, presented as the mean \pm SD of three independent experiments, indicate statistical significance, Δ $p < 0.001$, of the control vs. FRK; * $p < 0.05$, ** $p < 0.01$ and *** $p < 0.001$ indicate significance between the PEO and FRK treatment groups. Patchouli essential oil (PEO), forskolin (FRK), kojic acid (KA), tyrosinase (TYR), tyrosinase-related protein 1,2 (TRP-1,2), Glyceraldehyde 3-phosphate dehydrogenase (GAPDH), and non-significant (NS).

3.3. PEO Inhibits Mushroom Tyrosinase Activity

To explore whether PEO exhibited a direct inhibitory effect against the key enzyme in the melanogenesis process, a cell-free mushroom tyrosinase assay was conducted. The effect of PEO on mushroom tyrosinase activity is illustrated in Figure 3. We observed a dose-dependent inhibitory effect of PEO on the oxidation of L-tyrosine and L-DOPA by mushroom tyrosinase. The positive control, KA, demonstrated robust tyrosinase inhibition, as anticipated. However, KA displayed less inhibitory activity against mushroom tyrosinase (monophenolase) than PEO did at its maximum concentration (Figure 3A), although KA showed strong mushroom tyrosinase activity inhibition in the diphenolase phase (Figure 3B). Additionally, the IC_{50} values for PEO was determined to be 67.2 $\mu\text{g/mL}$ for L-tyrosine and 81.4 $\mu\text{g/mL}$ for L-DOPA, respectively. These results highlight the fact that PEO exhibits a potent inhibitory effect on mushroom tyrosinase activity.

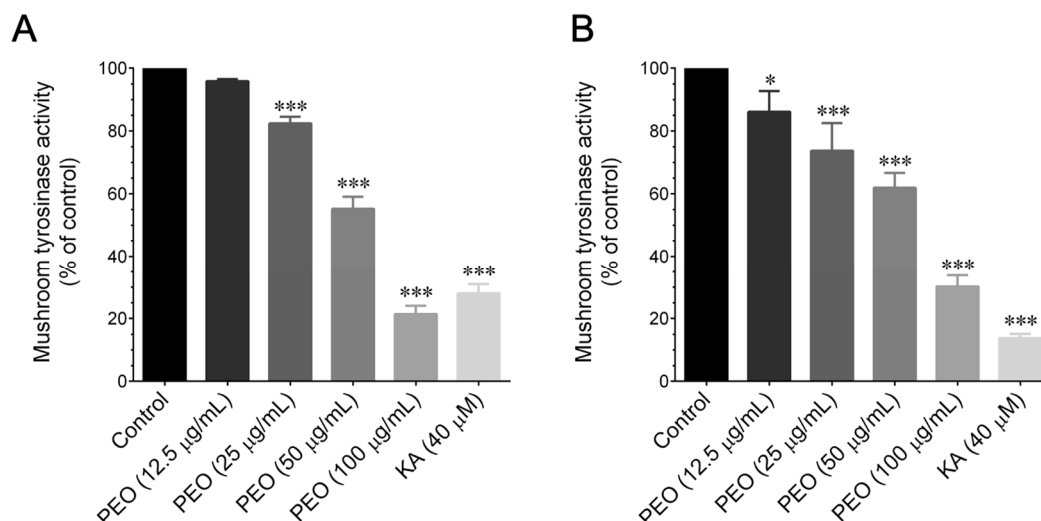


Figure 3. The inhibitory effects of PEO on mushroom tyrosinase activity. Mushroom tyrosinase (2000 U/mL) was incubated with the indicated concentrations of PEO for 10 min at room temperature prior to incubation with 15 mM of L-tyrosine (A) or L-DOPA (B) for 30 min. The results, presented as the mean \pm SD of three independent experiments, indicate statistical significance, * $p < 0.05$, and *** $p < 0.001$, of the control vs. PEO treatment groups. Patchouli essential oil (PEO) and kojic acid (KA).

3.4. PA Inhibits Melanin Biosynthesis in FRK-Induced B16-F10 Cells

Referring to a previous study by Cahyono et al. [16], it is evident that the chemical composition of patchouli oil comprises oxygenated sesquiterpenes and hydrocarbon sesquiterpenes, with patchouli alcohol being the predominant component, constituting 32.88% of patchouli oil. The second, third, and fourth primary compounds are δ -guaiene, α -guaiene, and α -patchoulene, comprising 21.60%, 18.78%, and 8.58% of patchouli oil, respectively. Therefore, we hypothesized that the notable skin-whitening property observed in PEO might be attributed to the presence of PA in its composition, considering it was identified as the primary component. Before investigating the anti-melanogenic activity of PA, an MTT assay was performed to assess its cytotoxicity. The results indicated that it had no cytotoxic effects on B16-F10 cells at dosages below 100 μ M. However, doses exceeding 100 μ M exhibited significant cytotoxicity (Figure 4A). Figure 4B illustrates the inhibitory activity of PA on melanin synthesis. The data suggest that PA can inhibit melanin synthesis in a dose-dependent manner, with its efficacy at a higher dose of 100 μ M being comparable to that of 40 μ M KA. The observed effect was further confirmed through FM staining. As shown in Figure 4C, cells treated with FRK displayed a significant increase in FM staining compared to control cells. However, cells treated with either PA or KA exhibited reduced FM staining, suggesting lower levels of intracellular melanin.

3.5. PA Inhibits FRK-Induced Cellular Tyrosinase Activity and Expression

To examine the mechanism through which PA diminishes melanin biosynthesis in B16-F10 cells, we assessed their cellular tyrosinase activity. According to the data presented in Figure 5A, there was a notable rise in cellular tyrosinase activity, reaching a level of 342.7%, following stimulation by FRK. Nevertheless, the addition of PA led to a decrease in cellular tyrosinase activity, with reductions of 250%, 220%, and 140% seen at concentrations of 25 μ M, 50 μ M, and 100 μ M, respectively. Moreover, the inhibitory potency of PA was found to be comparable to that of KA. The results imply that PA exhibits a potent inhibitory effect on intracellular tyrosinase activity. To enhance our understanding of PA's inhibitory effect on melanin synthesis and tyrosinase activity, our aim was to assess the impact of PA on the protein tyrosinase, which is involved in the regulation of melanogenesis. Immunofluorescence analysis revealed that, in comparison to control

cells, tyrosinase expression significantly increased upon FRK stimulation, as evidenced by a notable enhancement of green fluorescence in the subcellular region. Nevertheless, co-treatment with PA significantly decreased tyrosinase expression, with this reduction extending below the basal level (Figure 5B). Indeed, in comparison to KA, PA demonstrated a pronounced reduction in tyrosinase activity. In order to provide a more comprehensive understanding of the underlying mechanism responsible for the reduction of tyrosinase protein expression induced by PA, we conducted q-PCR analysis to evaluate the mRNA expression levels of tyrosinase, TRP-1, and TRP-2 in B16-F10 cells. According to the data presented in Figure 5C–E, it can be observed that, in cells stimulated by FRK, the mRNA expression levels of tyrosinase and TRP-1 exhibited a considerable rise of 4.2-fold and 3.5-fold, respectively. Unexpectedly, a concurrent administration of PA did not result in any changes in the levels of mRNA expression across all the doses that were examined. Furthermore, incubation with either FRK or PA did not induce any modulation in the TRP-1 expression in B16-F10 cells. The findings of this study indicate that the observed decrease in cellular tyrosinase activity caused by PA is likely a result of a direct inhibition of tyrosinase activity, rather than the modulation of its associated signaling system.

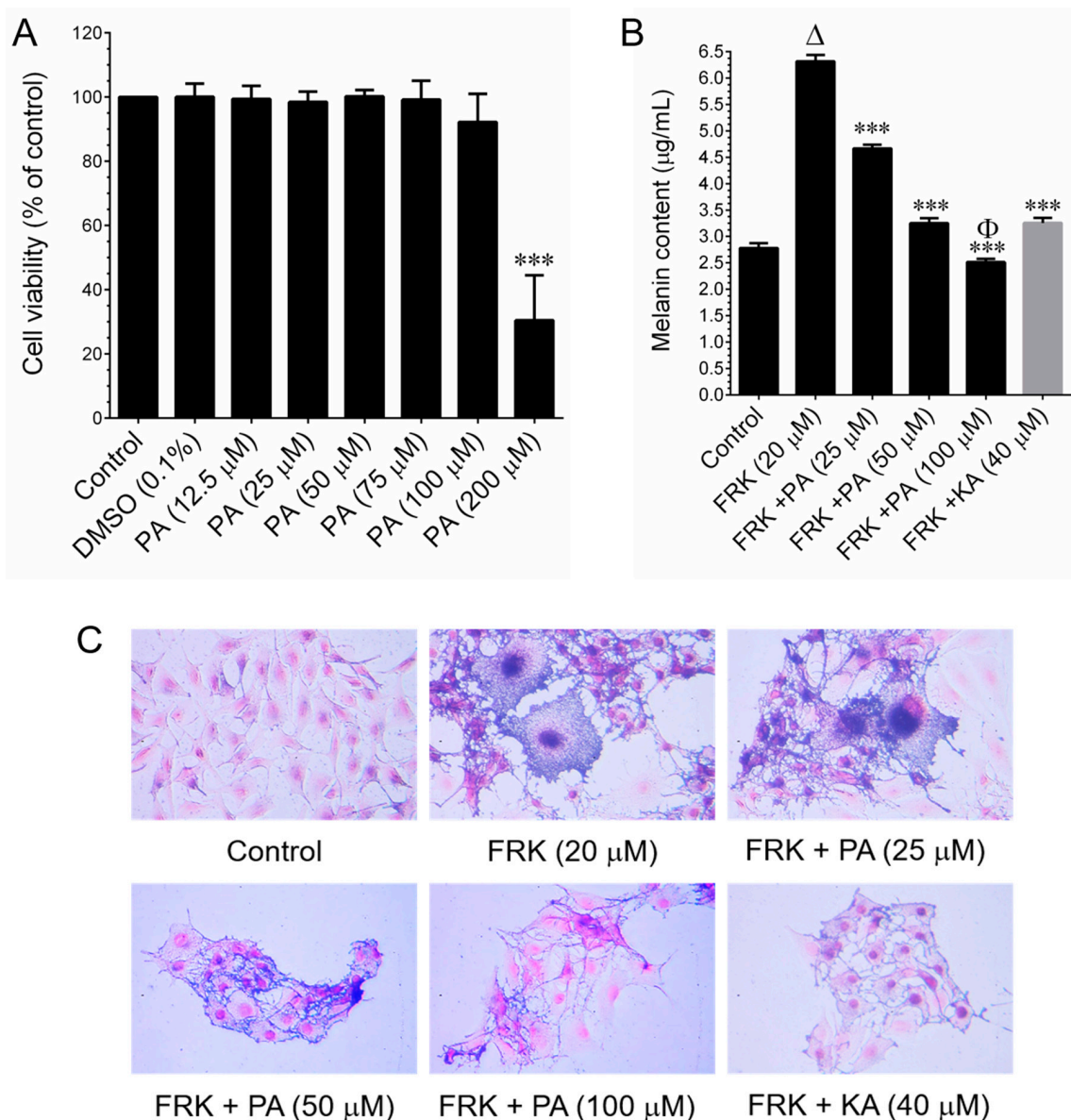


Figure 4. The effects of PA on melanin synthesis in B16-F10 cells. (A) Cells were incubated with increasing doses of PA (12.5–200 µM) for 48 h, and cell viability was assessed using an MTT colorimetric assay.

The results, presented as the mean \pm SD of three independent experiments, indicate statistical significance (** $p < 0.001$) when comparing the control and PA treatment groups. (B) Cells were treated with increasing doses of PA (25–100 μ M) or KA (40 μ M) in the presence of 20 μ M FRK for 48 h, and their melanin content was quantified from their total cell lysates. (C) Following a 48 h treatment with PA and FRK, cells were stained using Fontana–Masson staining to visualize their subcellular melanin content. The data, representing the mean \pm SD of three independent experiments, indicate statistical significance ($\Delta p < 0.001$ when comparing the control to FRK; $\Phi p < 0.05$ between the PA and control groups; ** $p < 0.001$ between the PA/KA and FRK treatment groups). Dimethyl sulfoxide (DMSO), patchouli alcohol (PA), forskolin (FRK), and kojic acid (KA).

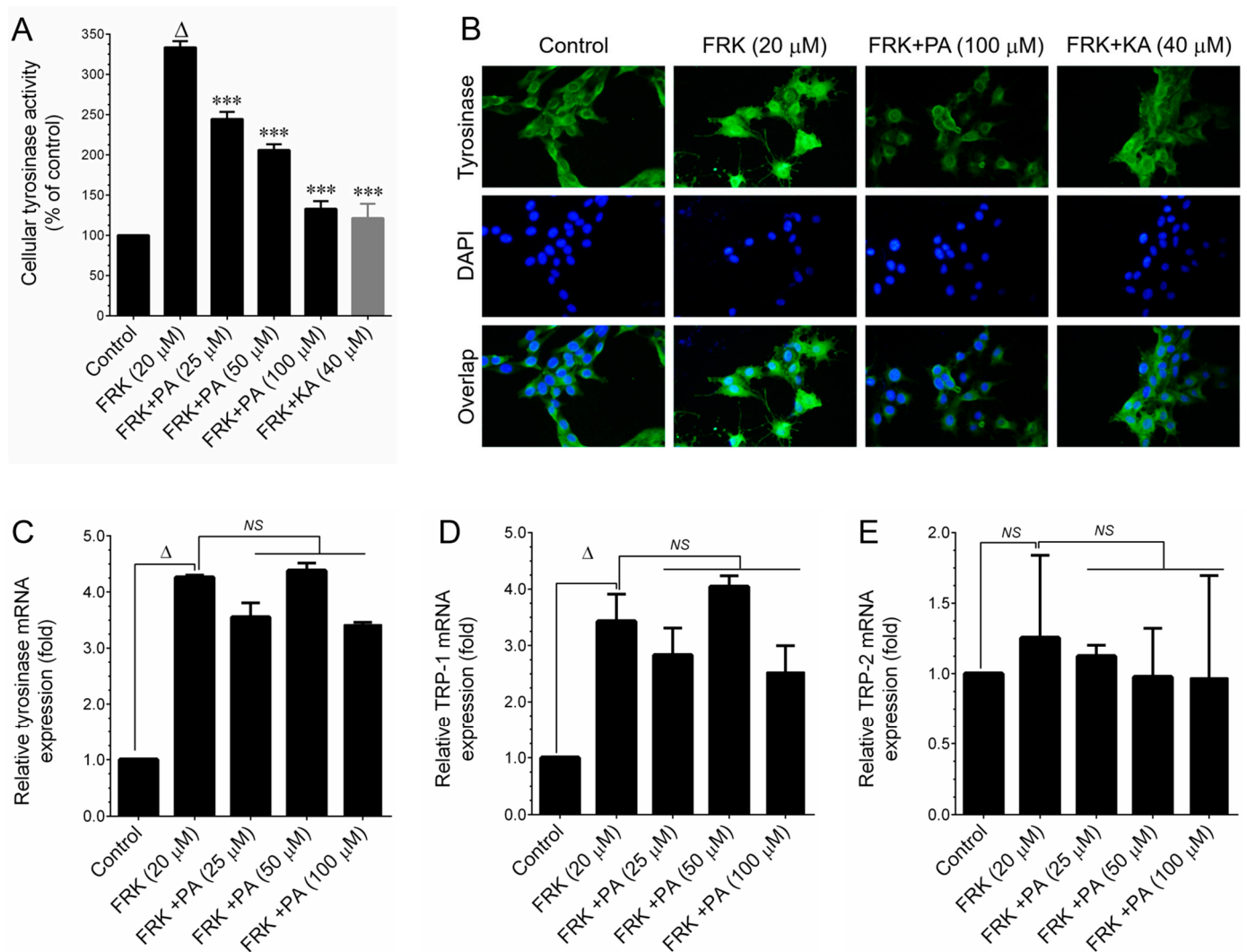


Figure 5. Effect of PA on FRK-induced cellular tyrosinase, tyrosinase proteins, and melanogenesis-regulatory genes in B16–F10 cells. Cells were treated with increasing concentrations of PA or KA and stimulated with FRK for 48 h. (A) Cellular tyrosinase activity was measured enzymatically, using L-DOPA as a substrate. The effects on L-DOPA oxidation velocity were measured at 492 nm. (B) The subcellular localization of tyrosinase protein expression was determined by immunofluorescence analysis. (C–E) Relative mRNA expression levels of tyrosinase, TRP-1, and TRP-2 were determined by q-PCR analysis. The data, representing the mean \pm SD of three independent experiments, indicate statistical significance ($\Delta p < 0.001$ when comparing the control to FRK; ** $p < 0.001$ between the PA and FRK treatment groups). Patchouli alcohol (PA), forskolin (FRK), kojic acid (KA), tyrosinase-related protein 1,2 (TRP-1,2), 4',6-diamidino-2-phenylindole (DAPI), and non-significant (NS).

3.6. PA Inhibits Mushroom Tyrosinase Activity

To investigate whether PA demonstrated a direct inhibitory effect against the pivotal enzyme in the melanogenesis process, a cell-free mushroom tyrosinase assay was conducted. The impact of PA on mushroom tyrosinase activity is depicted in Figure 6. Similar to PEO, we noted a dose-dependent inhibitory effect of PA on the oxidation of L-tyrosine (Figure 6A) and L-DOPA (Figure 6B) by mushroom tyrosinase. Furthermore, the IC_{50} values for PA were determined to be $49.4 \mu\text{M}$ for L-tyrosine and $39.6 \mu\text{M}$ for L-DOPA, respectively. These findings emphasize that PA demonstrates a potent inhibitory effect on mushroom tyrosinase activity.

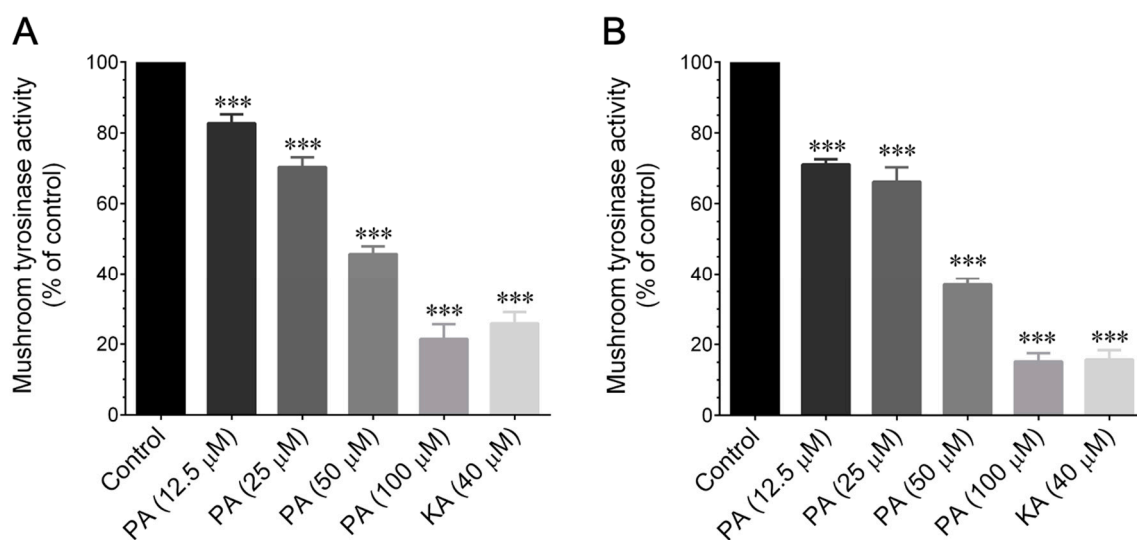


Figure 6. Inhibitory effects of PA on mushroom tyrosinase activity. Mushroom tyrosinase (2000 U/mL) was incubated with the indicated concentrations of PA for 10 min at room temperature prior to incubation with 15 mM of L-tyrosine (A) or L-DOPA (B) for 30 min. The results, presented as the mean \pm SD of three independent experiments, indicate statistical significances of *** $p < 0.001$ when comparing the control and PA treatment groups. Patchouli alcohol (PA), kojic acid (KA).

3.7. Molecular Docking

The investigation into the molecular interaction between human tyrosinase and the ligands of aromatic organic compounds revealed that all nine ligands exhibited a substantial amount of binding free energy. In general, hydrogen bonding is a complex mechanism, and the elimination of certain atoms involved in the hydrogen bonding process may enhance binding efficiency. Interestingly, we observed significant binding energy even in the absence of a single hydrogen bond in the docked pose (Figure 7). As all our ligands lack heteroatoms such as oxygen, nitrogen, sulfur, etc., there is no possibility of hydrogen bonds forming between the receptor and the ligands. However, the ligands δ -guaiene, α -guaiene, α -bulnesene, and seychellene exhibited greater binding free energy compared to the other ligands (-6.12 kcal/mol , -6.02 kcal/mol , -5.0 kcal/mol , and -5.97 kcal/mol , respectively). We hypothesize that their significant binding free energies are attributed to the formation of strong electrostatic interactions between the ligand and the receptor. All ligands exhibited electrostatic/Van der Waals attractions with amino acids. The ligand δ -guaiene, which has a high binding energy, interacted specifically with amino acids Arg:230, Leu:229, Lys:233, Pro:115, Tyr:226, and Pro:445 of the tyrosinase. Another ligand, α -guaiene, has nonphysical interactions with following amino acids: Leu:229, Lys:233, Arg:230, Tyr:226, Val:447, Pro:115, and Pro:445. Human tyrosinase possesses a functional site within the protein's 287–313 region. Our study aligns with these findings, as almost all ligands exhibited an attraction to numerous amino acids, the majority of which are situated between positions 187 and 313 of the receptor. In this study, all nine ligands were successfully superimposed onto the structure of the tyrosinase protein, revealing the

significant binding energy between them. Given that the ligands bind to the active site of the receptor protein, these findings suggest their potential to influence the mechanism of melanin synthesis.

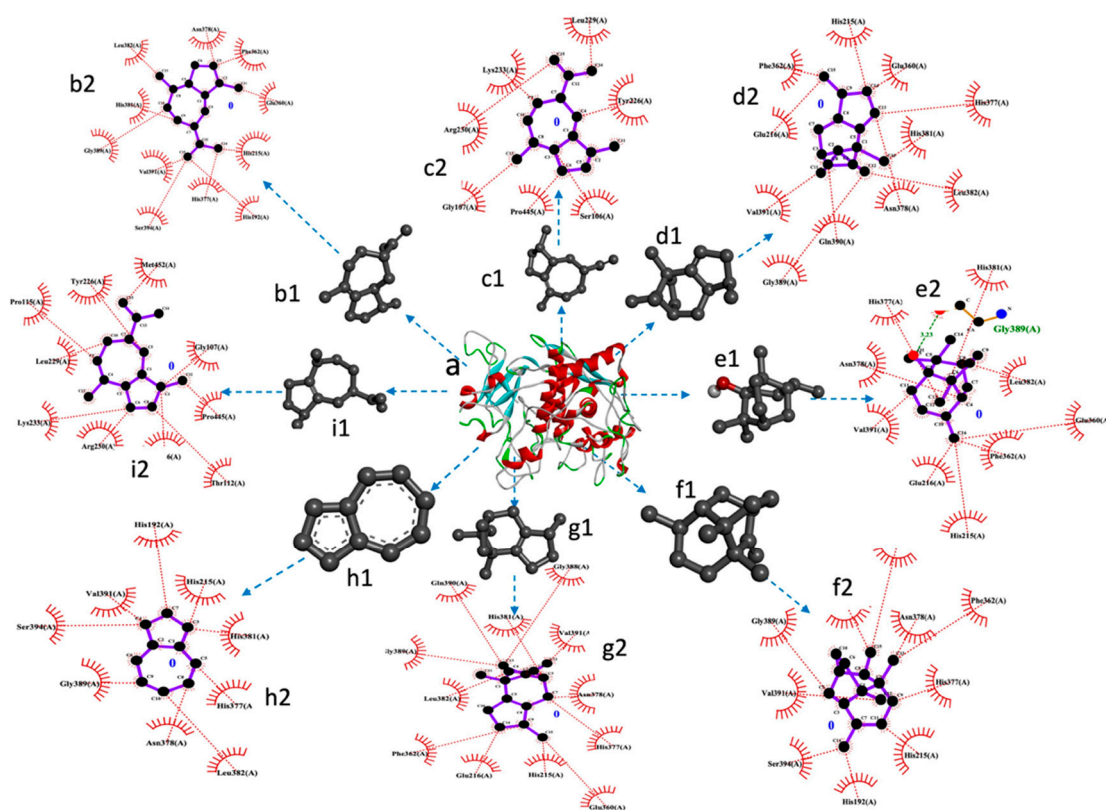


Figure 7. Molecular docking of tyrosinase with major components of PEO. (a) 3D structure of human tyrosinase (AF-L8B082-F1); (b1) 3D structure of α -bulnesene; (b2) docked pose of AF-L8B082-F1 and α -bulnesene; (c1) 3D structure of α -guaiene; (c2) docked pose of AF-L8B082-F1 and α -guaiene; (d1) 3D structure of β -patchoulene; (d2) docked pose of AF-L8B082-F1 and β -patchoulene; (e1) 3D structure of patchouli alcohol; (e2) docked pose of AF-L8B082-F1 and patchouli alcohol; (f1) 3D structure of seychellene; (f2) docked pose of AF-L8B082-F1 and seychellene; (g1) 3D structure of δ -patchoulene; (g2) docked pose of AF-L8B082-F1 and δ -patchoulene; (h1) 3D structure of azulene; (h2) docked pose of AF-L8B082-F1 and azulene; (i1) 3D structure of δ -guaiene; and (i2) docked pose of AF-L8B082-F1 and δ -guaiene.

4. Discussion

For over a millennium, essential oils have been utilized in pharmaceutical and cosmetic formulations, due to their diverse health benefits and preservative effect. Additionally, essential oils are widely recognized for their aromatic qualities, and, beyond fragrance, they have a spectrum of therapeutic properties [17]. This multifaceted nature proves to be a boon for the cosmetic industry when essential oils are integrated into their formulations. In recent years, essential oils (EOs) and essential oil components (EOCs) have gained significant popularity as ingredients in skincare products [18]. The increasing interest in utilizing these molecules in skincare formulations seeks to leverage their diverse biological properties, such as their antimicrobial, anti-inflammatory, and antioxidant effects [18]. This trend aims to contribute to maintaining youthful, healthy, and fresh skin while providing protection against environmental damage. The pharmacological potential of essential oils (EOs) derived from plants has been extensively studied in relation to their capacity to block melanin formation, making them a subject of significant interest as skin-lightening agents [19].

Pogostemon cablin has been extensively utilized in traditional Chinese medicine to address various ailments, particularly skin disorders. Notably, *P. cablin* holds a prominent position among the ten most commonly utilized traditional Chinese medicines within the context of skin beauty and care regimens [20]. Upon hydrodistillation, the dry leaves of *P. cablin* yield an essential oil known as patchouli essential oil (PEO). Cahyono et al. identified nine compounds in patchouli oil. The major compounds they reported included α -guaiene, α -patchoulene, δ -guaiene, and patchouli alcohol [16]. Fensia et al. [21] successfully isolated 13 compounds from patchouli oil, with patchouli alcohol identified as the major component. Furthermore, a comparative analysis of the chemical fingerprints of two *Pogostemon* species unveiled the presence of 26 compounds in *P. heyneanus* and 32 compounds in *P. cablin*. Notably, the primary compound in *P. cablin* was identified as being patchouli alcohol, constituting 38.3% of its compounds. Conversely, acetophenone dominated in *P. heyneanus*, comprising 51% of its compounds, with patchouli alcohol as the second major component at 14% [22]. Collectively, these studies suggest that patchouli alcohol, identified as one of the major chemical constituents of patchouli oil, plays a significant role in imparting its intense aromatic odor. Currently, PEO stands as a pivotal ingredient in cosmetic products, valued for its herbaceous notes and fixative properties. Pharmacological studies have revealed that PEO has diverse bioactive components, which demonstrate anti-allergic and anti-acne properties, and antibacterial effects on the skin, as well as anti-oxidative and anti-inflammatory benefits [23–25]. A previous study by Lin et al. [20] reported that the topical application of patchouli oil prevents the cutaneous photoaging induced by UV radiation in mice by enhancing the skin's antioxidant defense mechanism. However, the impact of PEO on cutaneous melanin biosynthesis was not explored. Likewise, patchouli alcohol (PA) is a tricyclic sesquiterpene widely utilized in the fragrance industry, in soaps, and in other cosmetic products [12,26]. Recent scientific investigations have documented with a broad spectrum of PA's bio-activities, including anti-influenza virus, anti-depressive, anti-nociceptive, vasorelaxation, lung and brain protection, anti-ulcerogenic, anti-colitis, prebiotic-like, anti-inflammatory, anti-cancer, and protective effects against metabolic diseases [24,27]. PA has been shown to offer potential skin health benefits. Kim et al. [28] demonstrated its ability to promote wound healing in obese mice. Additionally, another study by Feng et al. [29] illustrated that the topical application of PA protects mice skin from UV-induced premature skin aging. However, the skin-whitening/lightening effect of PA remains unexplored.

Melanin biosynthesis involves a series of sequential steps, encompassing receptor activation, intracellular cAMP production, the transcriptional activation of MITF, and the transcription of genes within the tyrosinase family [30]. In this study, we induced melanin synthesis in vitro using forskolin (FRK), a cAMP agonist known to trigger melanogenesis [30]. Subsequently, we investigated the inhibitory effects of PEO on melanin synthesis under these conditions. Our study revealed that treatment with PEO significantly inhibited melanin synthesis in B16-F10 cells. This finding aligns well with others' observations that essential oils from various sources, including *Alpinia nantoensis*, *Alpinia zerumbet*, *Cinnamomum cassia*, *Eucalyptus camaldulensis*, *Melaleuca quinquenervia*, *Calocedrus formosana*, and *Origanum ehrenbergii* [13,31–35], demonstrated robust melanin synthesis inhibition under conditions similar to those our in vitro experiments. Furthermore, essential oils exhibit the ability to inhibit melanin biosynthesis through two mechanisms [36]. This includes the direct inhibition of tyrosinase enzyme activity and the downregulation of the melanin biosynthesis pathway by modulating cellular signaling cascades. Tyrosinase family proteins, such as TYR, TRP-1, and TRP-2, play pivotal roles in melanin biosynthesis. Our study revealed that both PEO and PA significantly inhibited FRK-induced cellular tyrosinase activity. However, a noticeable reduction in TYR protein expression was observed only at a higher dose of both PEO and PA, while the levels of TRP-1 and TRP-2 remained unaffected. Furthermore, the FRK-induced elevation of TYR, TRP-1, and TRP-2 mRNA expression levels was unaltered by either PEO or PA. This observation suggests that PEO and PA

inhibit melanin biosynthesis not by altering signaling cascades, but possibly through the direct inhibition of tyrosinase activity.

Numerous essential oils have undergone extensive study with regard to their direct tyrosinase inhibition properties [19]. Momtaz et al. [37] stated that plant oils are abundant in compounds that include hydrophobic components, which can function as competitive inhibitors for the enzyme tyrosinase, thereby influencing melanin synthesis. This distinctive characteristic positions them as crucial ingredients in the development of skin-lightening agents, showcasing their potential to address and alleviate skin pigmentation issues. Similarly, numerous photo compounds have been investigated and demonstrated to possess direct tyrosinase inhibitory effects [38,39]. Hence, we aimed to investigate whether PEO or PA could modulate tyrosinase enzyme activity. A mushroom tyrosinase inhibitory assay was employed, as it is a widely used method for assessing the skin-whitening effects of candidate agents in a cell-free system. This is based on the rationale that tyrosinase serves as the limiting enzyme in melanin formation in the skin. Using this assay, we assessed the tyrosinase inhibitory effects of PEO and PA, utilizing L-tyrosine and L-DOPA as substrates. Our findings revealed that both PEO and PA inhibit mushroom tyrosinase activity in a cell-free system at both the monophenolase and diphenolase phases. This observation correlates with other studies that have suggested that several herbal extracts and phytochemicals can inhibit tyrosinase activity without affecting the upstream signaling cascades of tyrosinase production [14].

To further explore the interactions between enzymes and ligands, we conducted a molecular docking analysis. Typically, natural products and protein peptides with tyrosinase inhibitory activity contain high levels of hydrophobic (Trp, Phe, Gly, Val, Leu, Ile, Ala, Pro, and Met) and aromatic (Tyr, Trp, and Phe) amino acids [40]. Our docking analysis revealed that patchouli alcohol forms six hydrogen bonds with the tyrosinase enzyme at residues Leu382, Val392, His215, 377, 381, and Phe362. Previous studies have demonstrated that potent tyrosinase inhibitors bind to these residues [41]. Specifically, the amino acids His, Val, Thr, Met, and Leu are crucial interaction sites for tyrosinase inhibitors [42]. Additionally, various tyrosinase inhibitors, such as carvacrol derivatives, tyrosol derivatives, ketones, hesperetin, oxoethyl derivatives, and certain food peptides, have been found to inactivate the enzyme by interacting with these critical residues [43].

5. Conclusions

In conclusion, our investigation into the tyrosinase and melanin synthesis inhibitory effects of *Pogostemon cablin* essential oil (patchouli essential oil, PEO) and its primary bioactive compound, patchouli alcohol (PA), revealed significant and dose-dependent reductions in forskolin-induced melanin biosynthesis, cellular tyrosinase activity, and tyrosinase (TYR) protein expression. While the transcriptional levels of *TYR* and tyrosinase-related proteins (*TRP-1* and *TRP-2*) remained unaffected, the results provided positive indications that PEO and PA may directly interrupt the activity of the tyrosinase enzyme, leading to a reduction in melanin biosynthesis. Additional studies confirmed their inhibitory effects on mushroom tyrosinase activity, and an *in silico* molecular docking analysis suggested that PA might potently inhibit human tyrosinase activity. Collectively, these findings strongly suggest the potential of patchouli essential oil and its primary bioactive component, patchouli alcohol, as promising treatments for hyperpigmentary skin conditions and in the development of cosmetic products designed to lighten the skin. To the best of our knowledge, this is the first report of the skin-whitening effect of patchouli oil and its major bioactive component, patchouli alcohol. Nevertheless, further studies should be conducted to extend our understanding of their potential skin-whitening effects in *in vivo* models before considering their development as skin-whitening agents for cosmetic purposes. It is important to acknowledge that natural products often manifest their activities through the synergy of various compounds, and a singular substance is usually not solely responsible for the biological effects observed. Consequently, additional experiments should be conducted to explore patchouli alcohol's synergistic effects with the other major compounds in patchouli oil.

Author Contributions: Conceptualization, S.-Y.W. and K.J.S.K.; methodology, K.J.S.K.; software, M.C.; validation, K.J.S.K., M.C. and M.G.V.; formal analysis, K.J.S.K. and W.-T.L.; investigation, M.G.V.; resources, K.J.S.K.; data curation, K.J.S.K. and M.C.; writing—original draft preparation, K.J.S.K. and W.-T.L.; writing—review and editing, K.J.S.K. and S.-Y.W.; supervision, K.J.S.K.; project administration, K.J.S.K.; funding acquisition, K.J.S.K. All authors have read and agreed to the published version of the manuscript.

Funding: This research was funded by National Science and Technology Council, Taiwan, grant number (NSTC 111-2313-B-005-052-MY3), and the APC was funded by K.J.S.K.

Institutional Review Board Statement: Not applicable.

Informed Consent Statement: Not applicable.

Data Availability Statement: The data presented in this study are available on request from the corresponding author.

Conflicts of Interest: The authors declare no conflicts of interest.

References

1. Choi, H.; Ryu, I.Y.; Choi, I.; Ullah, S.; Jung, H.J.; Park, Y.; Jeong, Y.; Hwang, Y.; Hong, S.; Yoon, I.S.; et al. Novel anti-melanogenic compounds, (Z)-5-(Substituted Benzylidene)-4-thioxothiazolidin-2-one derivatives: In vitro and in silico insights. *Molecules* **2021**, *26*, 4963. [[CrossRef](#)] [[PubMed](#)]
2. Li, E.P.H.; Min, H.J.; Belk, R.W. Skin lightening and beauty in four asian cultures. In *NA—Advances in Consumer Research*; Lee, A.Y., Soman, D., Eds.; Association for Consumer Research: Duluth, MN, USA, 2008; Volume 35, pp. 444–449.
3. Cheng, A.D.; De La Garza, H.; Maymone, M.B.C.; Johansen, V.M.; Vashi, N.A. Skin-lightening products: Consumer preferences and costs. *Cureus* **2021**, *13*, e17245. [[CrossRef](#)] [[PubMed](#)]
4. Slominski, A.; Tobin, D.J.; Shibahara, S.; Wortsman, J. Melanin pigmentation in mammalian skin and its hormonal regulation. *Physiol. Rev.* **2004**, *84*, 1155–1228. [[CrossRef](#)] [[PubMed](#)]
5. Maranduca, M.A.; Branisteanu, D.; Serban, D.N.; Branisteanu, D.C.; Stoleriu, G.; Manolache, N.; Serban, I.L. Synthesis and physiological implications of melanic pigments. *Oncol. Let.* **2019**, *17*, 4183–4187. [[CrossRef](#)] [[PubMed](#)]
6. Plensdorf, S.; Livieratos, M.; Dada, N. Pigmentation disorders: Diagnosis and management. *Am. Fam. Physician* **2017**, *96*, 797–804. [[PubMed](#)]
7. Kim, Y.J.; Uyama, H. Tyrosinase inhibitors from natural and synthetic sources: Structure, inhibition mechanism and perspective for the future. *Cell Mol. Life Sci.* **2005**, *62*, 1707–1723. [[CrossRef](#)] [[PubMed](#)]
8. Hida, T.; Kamiya, T.; Kawakami, A.; Ogino, J.; Sohma, H.; Uhara, H.; Jimbow, K. Elucidation of melanogenesis cascade for identifying pathophysiology and therapeutic approach of pigmentary disorders and melanoma. *Int. J. Mol. Sci.* **2020**, *21*, 6129. [[CrossRef](#)] [[PubMed](#)]
9. Qian, W.; Liu, W.; Zhu, D.; Cao, Y.; Tang, A.; Gong, G.; Su, H. Natural skin-whitening compounds for the treatment of melanogenesis. *Exp. Ther. Med.* **2020**, *20*, 173–185. [[CrossRef](#)]
10. Couteau, C.; Coiffard, L. Overview of skin whitening agents: Drugs and cosmetic products. *Cosmetics* **2016**, *3*, 27. [[CrossRef](#)]
11. van Beek, T.A.; Joulain, D. The essential oil of patchouli, *Pogostemon cablin*: A review. *Flavor. Fragrance J.* **2018**, *33*, 6–51. [[CrossRef](#)]
12. Swamy, M.K.; Sinniah, U.R. A Comprehensive review on the phytochemical constituents and pharmacological activities of *Pogostemon cablin* Benth.: An aromatic medicinal plant of industrial importance. *Molecules* **2015**, *20*, 8521–8547. [[CrossRef](#)]
13. Kumar, K.J.S.; Vani, M.G.; Wu, P.C.; Lee, H.J.; Tseng, Y.H.; Wang, S.Y. Essential oils of *Alpinia nantoensis* retard forskolin-induced melanogenesis via ERK1/2-mediated proteasomal degradation of MITF. *Plants* **2020**, *9*, 1672. [[CrossRef](#)]
14. Chang, T.S. Natural melanogenesis inhibitors acting through the down-regulation of tyrosinase activity. *Materials* **2012**, *5*, 1661–1685. [[CrossRef](#)]
15. Elumalai, L.; Palaniyandi, S.; Anbazhagan, G.K.; Mohanam, N.; Munusamy, S.; G.K, S.R.; Pudukadu Munusamy, A.; Chinnasamy, M.; Ramasamy, B. Synthesis of biogenic cadmium sulfide nanoparticles (MR03-CdSNPs) using marine *Streptomyces kunmingensis*—MR03 for in-vitro biological determinations and in silico analysis on biofilm virulence proteins: A novel approach. *Environ. Res.* **2023**, *235*, 116698. [[CrossRef](#)]
16. Cahyono, E.; Rimawati, B.C.; Kusuma, E. Antidepressant activity of patchouli alcohol microcapsule. *J. Phys. Conf. Ser.* **2019**, *1321*, 022039. [[CrossRef](#)]
17. Sharmeen, J.B.; Mahomoodally, F.M.; Zengin, G.; Maggi, F. Essential oils as natural sources of fragrance compounds for cosmetics and cosmeceuticals. *Molecules* **2021**, *26*, 666. [[CrossRef](#)]
18. Guzmán, E.; Lucia, A. Essential oils and their individual components in cosmetic products. *Cosmetics* **2021**, *8*, 114. [[CrossRef](#)]
19. Aumeeruddy-Elalfi, Z.; Gurib-Fakim, A.; Mahomoodally, M.F. Kinetic studies of tyrosinase inhibitory activity of 19 essential oils extracted from endemic and exotic medicinal plants. *S. Afr. J. Bot.* **2016**, *103*, 89–94. [[CrossRef](#)]

20. Lin, R.F.; Feng, X.X.; Li, C.W.; Zhang, X.J.; Yu, X.T.; Zhou, J.Y.; Zhang, X.; Xie, Y.L.; Su, Z.R.; Zhan, J.Y. Prevention of UV radiation-induced cutaneous photoaging in mice by topical administration of patchouli oil. *J. Ethnopharmacol.* **2014**, *154*, 408–418. [[CrossRef](#)] [[PubMed](#)]
21. Souhoka, F.; Al Aziz, A.; Nazudin, N. Patchouli oil isolation and identification of chemical components using GC-MS. *Indo. J. Chem. Res.* **2020**, *8*, 108–113. [[CrossRef](#)]
22. Murugan, R.; Mallavarapu, G.R.; Padmashree, K.V.; Rao, R.R.; Livingstone, C. Volatile oil composition of *Pogostemon heyneanus* and comparison of its composition with patchouli oil. *Nat. Prod. Commun.* **2010**, *5*, 1961–1964. [[CrossRef](#)]
23. Fatima, S.; Farzeen, I.; Ashraf, A.; Aslam, B.; Ijaz, M.U.; Hayat, S.; Sarfraz, M.H.; Zafar, S.; Zafar, N.; Unuofin, J.O.; et al. A comprehensive review on pharmacological activities of pachypodol: A bioactive compound of an aromatic medicinal plant *Pogostemon cablin* Benth. *Molecules* **2023**, *28*, 3469. [[CrossRef](#)]
24. Lee, H.S.; Lee, J.; Smolensky, D.; Lee, S.H. Potential benefits of patchouli alcohol in prevention of human diseases: A mechanistic review. *Int. Immunopharmacol.* **2020**, *89*, 107056. [[CrossRef](#)]
25. Thakur, A. Therapeutic potential of *Pogostemon cablin* herb: A comprehensive review. *Pham Pat. Anal.* **2022**, *11*, 213–224. [[CrossRef](#)]
26. Bhatia, S.P.; Letizia, C.S.; Api, A.M. Fragrance material review on patchouli alcohol. *Food Chem. Toxicol.* **2008**, *46*, S255–S256. [[CrossRef](#)] [[PubMed](#)]
27. Hu, G.; Peng, C.; Xie, X.; Zhang, S.; Cao, X. Availability, pharmaceutics, security, pharmacokinetics, and pharmacological activities of patchouli alcohol. *Evid. Based Complement. Alternat Med.* **2017**, *2017*, 4850612. [[CrossRef](#)]
28. Kim, T.J.; Pyun, D.H.; Park, S.Y.; Lee, H.J.; Abd El-Aty, A.M.; Song, J.H.; Shin, Y.K.; Jeong, J.H.; Jung, T.W. Patchouli alcohol improves wound healing in high fat diet-fed mice through AMPK-mediated suppression of inflammation and TGF β 1 signaling. *Biochem. Biophys. Res. Commun.* **2021**, *561*, 136–142. [[CrossRef](#)] [[PubMed](#)]
29. Feng, X.X.; Yu, X.T.; Li, W.J.; Kong, S.Z.; Liu, Y.H.; Zhang, X.; Xian, Y.F.; Zhang, X.J.; Su, Z.R.; Lin, Z.X. Effects of topical application of patchouli alcohol on the UV-induced skin photoaging in mice. *Eur. J. Pharmacol. Sci.* **2014**, *63*, 113–123. [[CrossRef](#)]
30. D’Mello, S.A.; Finlay, G.J.; Baguley, B.C.; Askarian-Amiri, M.E. Signaling pathways in melanogenesis. *Int. J. Mol. Sci.* **2016**, *17*, 1144. [[CrossRef](#)] [[PubMed](#)]
31. Tu, P.T.; Tawata, S. Anti-oxidant, anti-aging, and anti-melanogenic properties of the essential oils from two varieties of *Alpinia zerumbet*. *Molecules* **2015**, *20*, 16723–16740. [[CrossRef](#)]
32. Chou, S.T.; Chang, W.L.; Chang, C.T.; Hsu, S.L.; Lin, Y.C.; Shih, Y. *Cinnamomum cassia* essential oil inhibits α -MSH-induced melanin production and oxidative stress in murine B16 melanoma cells. *Int. J. Mol. Sci.* **2013**, *14*, 19186–19201. [[CrossRef](#)]
33. Huang, H.C.; Ho, Y.C.; Lim, J.M.; Chang, T.Y.; Ho, C.L.; Chang, T.M. Investigation of the anti-melanogenic and antioxidant characteristics of *Eucalyptus camaldulensis* flower essential oil and determination of its chemical composition. *Int. J. Mol. Sci.* **2015**, *16*, 10470–10490. [[CrossRef](#)]
34. Hsiao, W.W.; Kumar, K.J.S.; Lee, H.J.; Tsao, N.W.; Wang, S.Y. Anti-melanogenic activity of *Calocedrus formosana* wood essential oil and its chemical composition analysis. *Plants* **2021**, *11*, 62. [[CrossRef](#)] [[PubMed](#)]
35. Chao, W.W.; Su, C.C.; Peng, H.Y.; Chou, S.T. *Melaleuca quinquenervia* essential oil inhibits α -melanocyte-stimulating hormone-induced melanin production and oxidative stress in B16 melanoma cells. *Phytomedicine* **2017**, *34*, 191–201. [[CrossRef](#)] [[PubMed](#)]
36. Huang, H.-C.; Wang, H.-F.; Yih, K.-H.; Chang, L.-Z.; Chang, T.-M. The dual antimelanogenic and antioxidant activities of the essential oil extracted from the leaves of *Acorus macrospadiceus* (Yamamoto) F. N. Wei et Y. K. Li. *Evid. Based Complement. Alternat Med.* **2012**, *2012*, 781280. [[CrossRef](#)] [[PubMed](#)]
37. Momtaz, S.; Mapunya, B.M.; Houghton, P.J.; Edgerly, C.; Hussein, A.; Naidoo, S.; Lall, N. Tyrosinase inhibition by extracts and constituents of *Sideroxylon inerme* L. stem bark, used in South Africa for skin lightening. *J. Ethnopharmacol.* **2008**, *119*, 507–512. [[CrossRef](#)] [[PubMed](#)]
38. Hassan, M.; Shahzadi, S.; Kloczkowski, A. Tyrosinase inhibitors naturally present in plants and synthetic modifications of these natural products as anti-melanogenic agents: A review. *Molecules* **2023**, *28*, 378. [[CrossRef](#)] [[PubMed](#)]
39. Zolghadri, S.; Bahrami, A.; Hassan Khan, M.T.; Munoz-Munoz, J.; Garcia-Molina, F.; Garcia-Canovas, F.; Saboury, A.A. A comprehensive review on tyrosinase inhibitors. *J. Enzyme Inhib. Med. Chem.* **2019**, *34*, 279–309. [[CrossRef](#)] [[PubMed](#)]
40. Song, Y.; Chen, S.; Li, L.; Zeng, Y.; Hu, X. The hypopigmentation mechanism of tyrosinase inhibitory peptides derived from food proteins: An overview. *Molecules* **2022**, *27*, 2710. [[CrossRef](#)]
41. Chang, T.S. An updated review of tyrosinase inhibitors. *Int. J. Mol. Sci.* **2009**, *10*, 2440–2475. [[CrossRef](#)]
42. Ren, Z.; Li, Q.; Shen, Y.; Meng, L. Intrinsic relative preference profile of pan-kinase inhibitor drug staurosporine towards the clinically occurring gatekeeper mutations in Protein Tyrosine Kinases. *Comput. Biol. Chem.* **2021**, *94*, 107562. [[CrossRef](#)] [[PubMed](#)]
43. Mohammadsadeghi, N.; Mahdavi, A.; Saadati, F.; Mohammadi, F. In silico and in vitro studies of novel derivatives of tyrosol and raspberry ketone as the mushroom tyrosinase inhibitors. *Food Chem.* **2023**, *424*, 136413. [[CrossRef](#)] [[PubMed](#)]

Disclaimer/Publisher’s Note: The statements, opinions and data contained in all publications are solely those of the individual author(s) and contributor(s) and not of MDPI and/or the editor(s). MDPI and/or the editor(s) disclaim responsibility for any injury to people or property resulting from any ideas, methods, instructions or products referred to in the content.